Frontiers of Physics
https://doi.org/10.1007/s11467-021-1072-y
Front. Phys.
16(5), 53504 (2021)

RESEARCH ARTICLE

Toplayer-dependent crystallographic orientation imaging in the bilayer two-dimensional materials with transverse shear microscopy

Sabir Hussain[1,2,4,*], Rui Xu[1,*], Kunqi Xu[3], Le Lei[1], Shuya Xing[1], Jianfeng Guo[1], Haoyu Dong[1], Adeel Liaqat[2,4], Rashid Iqbal[2,4], Muhammad Ahsan Iqbal[2,4], Shangzhi Gu[1], Feiyue Cao[1], Yan Jun Li[5], Yasuhiro Sugawara[5], Fei Pang[1], Wei Ji[1], Liming Xie[2,4], Shanshan Chen[1,†], Zhihai Cheng[1,‡]

[1] *Beijing Key Laboratory of Optoelectronic Functional Materials & Micro-nano Devices, Department of Physics, Renmin University of China, Beijing 100872, China*
[2] *CAS Key Laboratory of Standardization and Measurement for Nanotechnology, CAS Center for Excellence in Nanoscience, National Center for Nanoscience and Technology, Beijing 100190, China*
[3] *Key Laboratory of Inorganic Functional Materials and Devices, Shanghai Institute of Ceramics, Chinese Academy of Sciences, Shanghai 200050, China*
[4] *University of Chinese Academy of Sciences, Beijing 100039, China*
[5] *Department of Applied Physics, Graduate School of Engineering, Osaka University, 2-1 Yamadaoka, Suita, Osaka 565-0871, Japan*
Corresponding authors. E-mail: †schen@ruc.edu.cn, ‡zhihaicheng@ruc.edu.cn
Received February 17, 2021; accepted April 19, 2021

Nanocontact properties of two-dimensional (2D) materials are closely dependent on their unique nanomechanical systems, such as the number of atomic layers and the supporting substrate. Here, we report a direct observation of toplayer-dependent crystallographic orientation imaging of 2D materials with the transverse shear microscopy (TSM). Three typical nanomechanical systems, MoS_2 on the amorphous SiO_2/Si, graphene on the amorphous SiO_2/Si, and MoS_2 on the crystallized Al_2O_3, have been investigated in detail. This experimental observation reveals that puckering behaviour mainly occurs on the top layer of 2D materials, which is attributed to its direct contact adhesion with the AFM tip. Furthermore, the result of crystallographic orientation imaging of MoS_2/SiO_2/Si and MoS_2/Al_2O_3 indicated that the underlying crystalline substrates almost do not contribute to the puckering effect of 2D materials. Our work directly revealed the top layer dependent puckering properties of 2D material, and demonstrate the general applications of TSM in the bilayer 2D systems.

Keywords 2D materials, toplayer-dependent crystallographic orientation imaging, nanomechanical contact properties, transverse shear microscopy

Following the discovery of graphene prepared by the micromechanical exfoliation technique [1], much research intension has been paid on the two-dimensional (2D) [2–7] material due to its superior characteristic properties, including excellent physical [8, 9], mechanical [10, 11], chemical [12, 13], electronic and optoelectronic properties [14–17]. One of the intriguing advantages of the 2D layered material is that their isotropic properties can be converted to be anisotropic, which results from the breaking symmetry owing to their intrinsic puckering behaviors. The puckering effect of 2D materials is due to the out-of-plane elastic deformation and the bending stiffness, and have attracted wide research interest [18, 19]. The anisotropies of 2D material exerted powerful influences on the ultrathin flexible nano-electromechanical and thermal devices [20].

Progress in the general understanding of isotropic to anisotropic relationships in 2D ultra-thin films requires experimental tools capable of imaging the details. Nanomechanical deformation has been extensively investigated by the atomic force microscopy (AFM) indentation experiments on suspended films [21–23]. Based on AFM platform [24–27], friction force microscopy (FFM) and transverse shear microscopy (TSM), as the derivative mode of contact AFM [28–32], now have been widely used to study the elastic deformation [19, 31], crystal structure [28], surficial ripples of 2D materials [8, 34, 35] and so on. Such studies have revealed an important phenomenon in which nanomechanical contact behavior could be dependent on the number of layers and substrates. While this layer-dependent transient phenomena in 2D materials on different supporting substrates has not been experimentally investigated.

Here, we focused experimental investigation on the sur-

*These two authors contributed equally to this work.
arXiv: 2105.09887. This article can also be found at http://journal.hep.com.cn/fop/EN/10.1007/s11467-021-1072-y.

© Higher Education Press 2021

face layer-dependent puckering behavior of 2D materials through the extensive TSM characterization for their crystallographic orientation imaging. First, we directly verify that the puckering effect mainly occurs on the top layer of 2D systems through the exclusive crystallographic orientations of the top layer of MoS_2 on the SiO_2/Si substrate. Second, the growth position of the adlayer graphene was definitely determined below the first layer during the CVD growth process by a combination of TSM and scanning Kelvin probe microscopy (SKPM) measurements. Finally, the TSM method was further generalized to realize the crystallographic orientation imaging of MoS_2 monolayer grown on the crystallized Al_2O_3 substrate.

All of the AFM measurements were conducted using an Asylum research AFM system (MFP-3D infinity). Both FFM and TSM are the derivative modes of contact AFM mode, as illustrated in Fig. 1. For the 2D thin films, during the contact AFM scanning, the film shows puckering effect around the moving AFM tip, as shown in Fig. 1(b). The puckered geometry induces the film to vertical relax at the front edge of the moving tip and simultaneously stretch the rear region of the moving tip. For FFM, the scan direction of the AFM tip is perpendicular to the long axis of the AFM cantilever, and then the friction property of the sample was obtained by detecting the torsion signal of the cantilever. For TSM, the scan direction of the AFM tip is parallel to the long axis of the cantilever, and then the shear property of the sample was obtained by detecting the torsion signal of the cantilever. For the 2D materials, the FFM measurements have shown that the friction force increases with the decreased thin film thickness due to the enhanced puckering effect. This puckering effect also enabled the TSM method to successfully image the orientation of the crystalline domains in star-shape MoS_2 monolayer flakes in our previously reported work [27]. While until now, it is still not clear about the toplayer-dependent puckering effect, and more experimental work should be performed to deeply understand this unique and typical nanomechanical behavior of 2D materials.

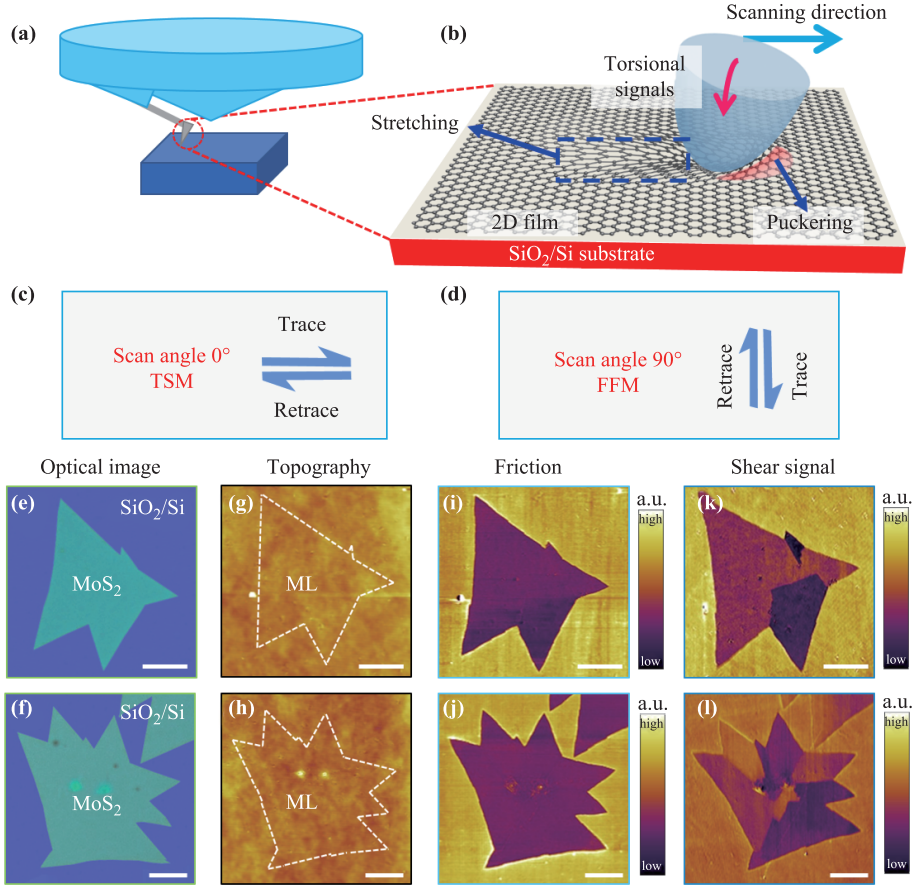


Fig. 1 FFM and TSM measurements of MoS_2 monolayer flakes on the SiO_2/Si substrate. **(a–d)** Schematic diagram illustrating the working mechanism of TSM and FFM on the thin 2D materials. The mechanical model illustrates the puckering behavior of thinfilm deformed by the loading and lateral force of the moving AFM tip. The scanning direction is perpendicular (parallel) to the cantilever axis in FFM (TSM). **(e–h)** Optical (e, f) and topography (g, h) images of two MoS_2 flakes without any crystalline grain contrast. The corresponding **(i, j)** friction (FFM) and **(k, l)** shear (TSM) signal images. Several grains in MoS_2 flakes are clearly resolved in the TSM images, but not in the FFM images. The scale bars are all 6 μm.

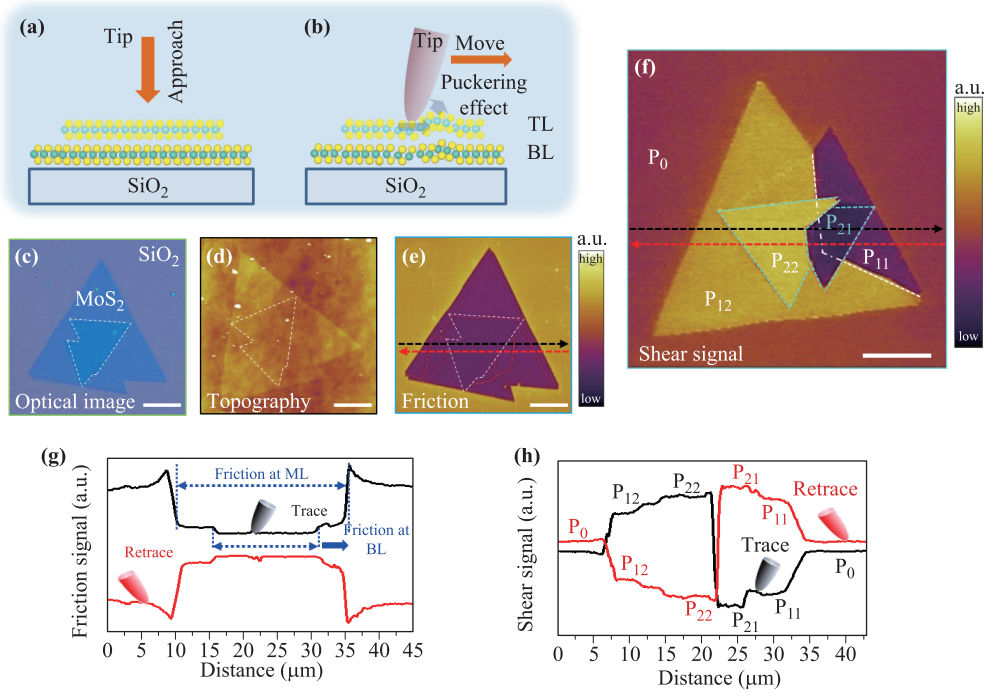


Fig. 2 Layer-dependent puckering effect of bilayer MoS_2 flake via FFM and TSM. **(a, b)** Schematic model illustrating the puckering effect mostly occurred on the top layer (TL) of MoS_2 rather than bottom layer (BL). **(c–f)** The optical (c), AFM topography (d), FFM (e) and TSM (f) images of bilayer MoS_2 on the SiO_2/Si substrate. The different MoS_2 grains are marked as P_{11} and, P_{12} for the bottom monolayer, P_{21} and P_{22} for the top layer of bilayer MoS_2. The amorphous SiO_2/Si substrate is marked as P_0. **(g, h)** The line profiles of friction (g) and shear (h) signals in the trace and retrace directions marked by black and red line in (e) and (f). The scale bars are all 8 μm.

First, the atomically thin CVD grown MoS_2 monolayer flakes were characterized by FFM and TSM imaging, as shown in Fig. 1. No crystalline differentiated contrast was observed in both optical and AFM topography images of MoS_2 monolayer flakes on the SiO_2/Si substrate [7]. Strain can induce the transformation from isotropy to

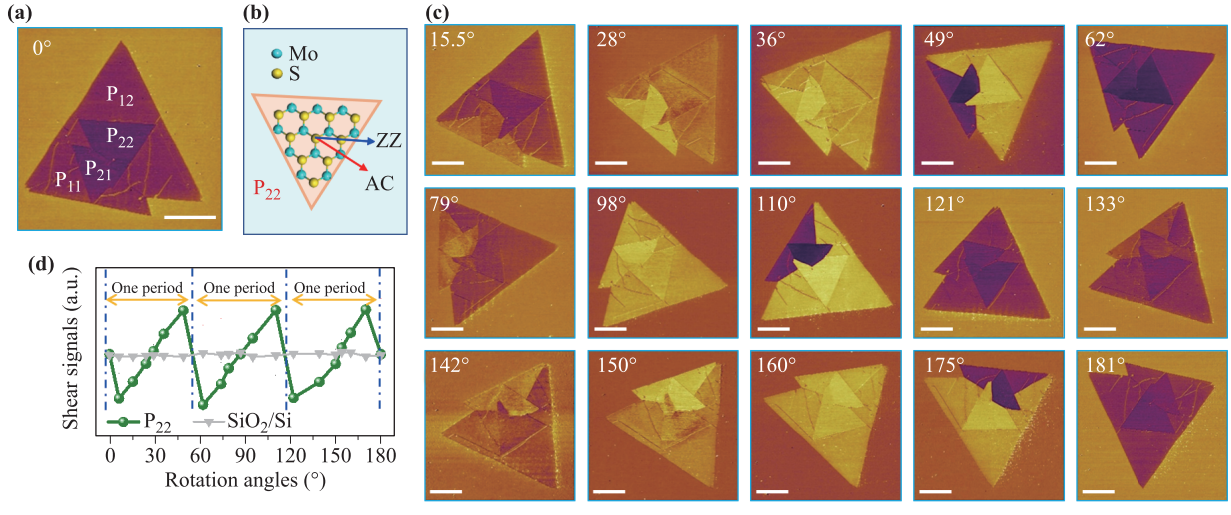


Fig. 3 Crystallography orientation dependency of the MoS_2 bilayer flake. **(a–c)** Crystallographic labels for the AC and ZZ orientations of MoS_2. Every grain is given an identifier of P_{11} and P_{12} for the bottom monolayer, P_{21} and P_{22} for the top layer of bilayer MoS_2. TSM images obtained by rotating the sample in clockwise direction. All the images use the same color contrast. The scale bars are all 8 μm. **(d)** Shear signal *vs* rotation angle curves obtained by randomly selecting P_{22} domains with the underlying amorphous SiO_2/Si substrate.

anisotropy of both in-plane normal tension stress and shear stiffness, but shear stiffness exhibits much greater anisotropy [31]. Here, even enhanced by the puckering effect (strain applied by probe), the FFM signals still do not reveal any significant contrast dependence on the crystallographic orientations on the grains due to their almost isotropic stress-strain mechanical behavior. While the clearly crystalline grains were clearly resolved in the TSM images through the anisotropic shear-strain mechanical behavior. The reason for the difference of imaging contrast between FFM and TSM was discussed in our previous work [31].

In order to investigate the toplayer-dependent puckering effect, we further perform the systematic AFM characterization on the bilayer MoS_2 flake made of two bottom layer grains and two top layer grains, as shown in Fig. 2. Due to the van der Walls (vdW) interactions between the top and bottom layer, the adhesion and puckering effect will most occur between the AFM tip and the top layer when the AFM tip approach, contact and move on the top layer [Figs. 2(a) and (b)]. Figure 2(c) and (d) show the optical and AFM topography images of the bilayer MoS_2 flakes. The bilayer areas can be clearly resolved and were marked by the white dashed lines.

Figure 2(e) shows the FFM images of this bilayer MoS_2 flake. No crystalline differentiated contrast was observed on both top and bottom layer grains. While it is noted that the friction signal on the bilayer area is slightly lower on the monolayer area, as shown in Fig. 2(g), which is in consistent with the previously reports in 2D materials [30, 38–41]. Figure 2(f) shows the TSM images of this bilayer MoS_2 flake. Both the top layer grains (P_{21}

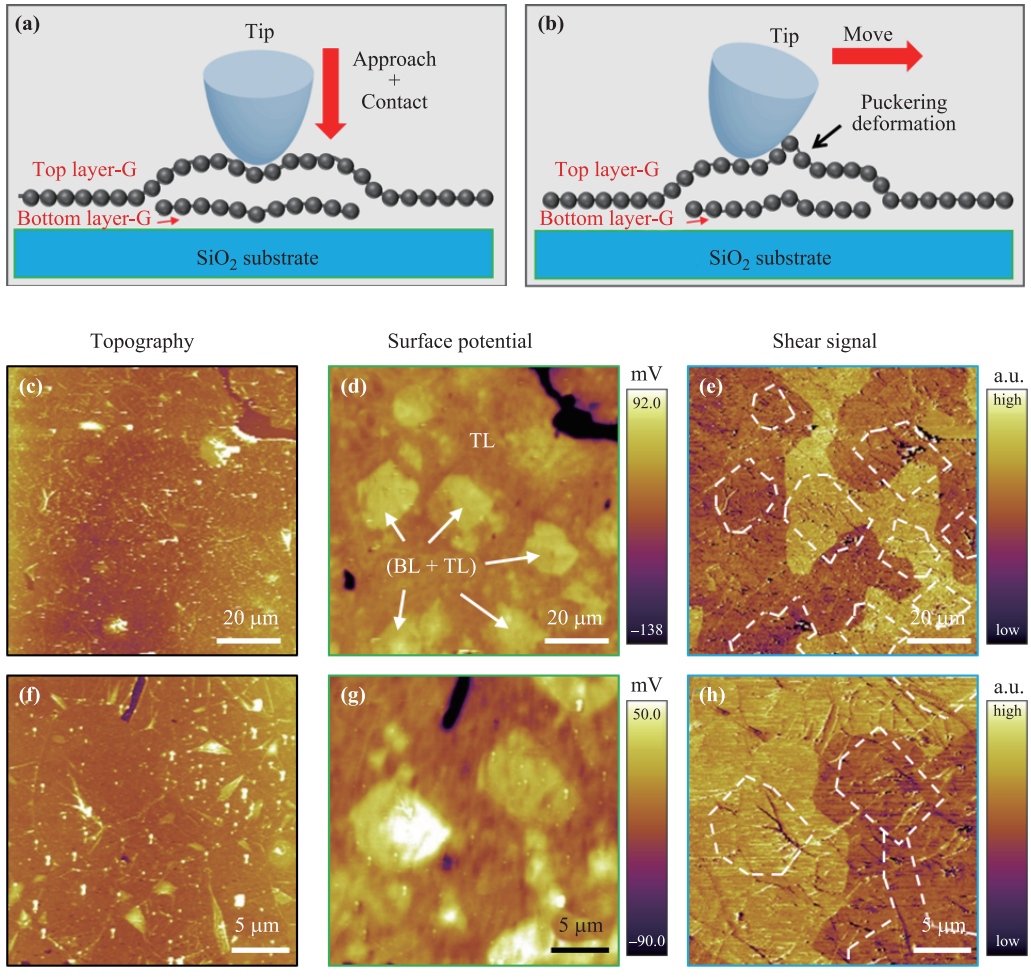


Fig. 4 AFM characterization of the CVD-grown bilayer graphene film transferred on the SiO_2/Si substrate. **(a, b)** The schematic diagram of the bilayer graphene film with the second layer grown below the first layer. The puckering effect mostly happened on the top layer (TL) of graphene rather than bottom layer (BL). **(c–h)** AFM topography (c, f), SKPM surface potential (d, g) and TSM shear signal (e, h) images of the bilayer graphene transferred on the SiO_2/Si substrate. Both scratches and wrinkles are observed in the topography images due to the transfer process, and the bilayer graphene area could not be determined by the topography images. The bilayer graphene area is determined by its higher surface potential than the monolayer. The grains of top layer graphene are clearly determined in the TSM images. The bottom second layers are marked by white dashed lines in (e) and (f).

and P_{22}) and the bottom layer grains (P_{11} and P_{12}) were clearly resolved in the TSM image. The P_{21} and P_{11} grains are in a near-pristine 2H stacking. The top layer grain of P_{22} shows almost the identical shear signal with the bottom layer grain of P_{12} due to their pristine 2H stacking with the same but inversion-asymmetry crystallographic orientation. Since the vdW interaction between the top and the bottom MoS_2 layer is less than the bonding between bottom MoS_2 layer and substrate, the difference between shear signals (the trace and retrace) of top layer is larger than bottom layer [Fig. 2(h)]. It is noted that the top layer grain of P_{21} (and P_{22}) is stacked over both the bottom layer grains of $P_{11}(P_{12})$, while no shear contrast was observed within the grain of P_{21} and P_{22}. This result directly demonstrates that the puckering effect mostly happened on the top layer, then the corresponding puckering-induced shear signal in the bottom grains should be very small in contrast to the top layer grain.

It is necessary to further investigate whether the anisotropic domains of the top layer grains depend on the crystallographic orientation in the TSM images. In Figs. 3(a) and (b), the crystallographic orientation (armchair and zigzag) of evert grain could be determined according to their primitive growth zigzag edges. By systematic TSM characterization with a series of clockwise rotations Fig. 3(c)], the periods of 60° of the shear signals with the rotation angle are presented [Fig. 3(d)], which is consistent with the monolayer MoS_2 in our previous work [31]. There is an interesting phenomenon that a singularity (a jump in value) exists in the zz orientation [~60°, 120° and 180°]. This phenomenon can be explained by shear stiffness anisotropy along zz orientation and AC orientation. Under the same transverse deformation, a greater restoring force results in increasing lateral torsion of the cantilever near the zz direction. The amorphous SiO_2/Si does not show any obvious dependency on the rotation angle. These results further confirm our ideas on the toplayer-pendent crystallographic orientation imaging, also demonstrate the general application of TSM to determine the crystallographic orientations of 2D materials, especially in the twisted bilayer or few-layer systems.

The toplayer-dependent TSM characterization can also be used to determine the special growth mode of bilayer graphene in combination with the SKPM measurements, as shown in Fig. 4. Figures 4(a) and (b) schematically show that the adhesion/puckering effect between the static /moving AFM tip and 2D layers are mostly emerge in the contacted top layer graphene. Figures 4(c) and (f) shows the AFM topography images of the bilayer graphene films transferred on the SiO_2/Si substrates (See details in supporting information). It is clearly that the bilayer graphene regions were not resolved in the topography images. Figures 4(d) and (g) show the corresponding surface potential of the bilayer graphene films obtained by the SKPM measurements. The bilayer and monolayer graphene regions were clearly distinguished by their different surface potentials and in good agreement with previously reported work [36]. To further determine whether the second growth layer is underlying the first layer or not, we perform the TSM characterization of the graphene

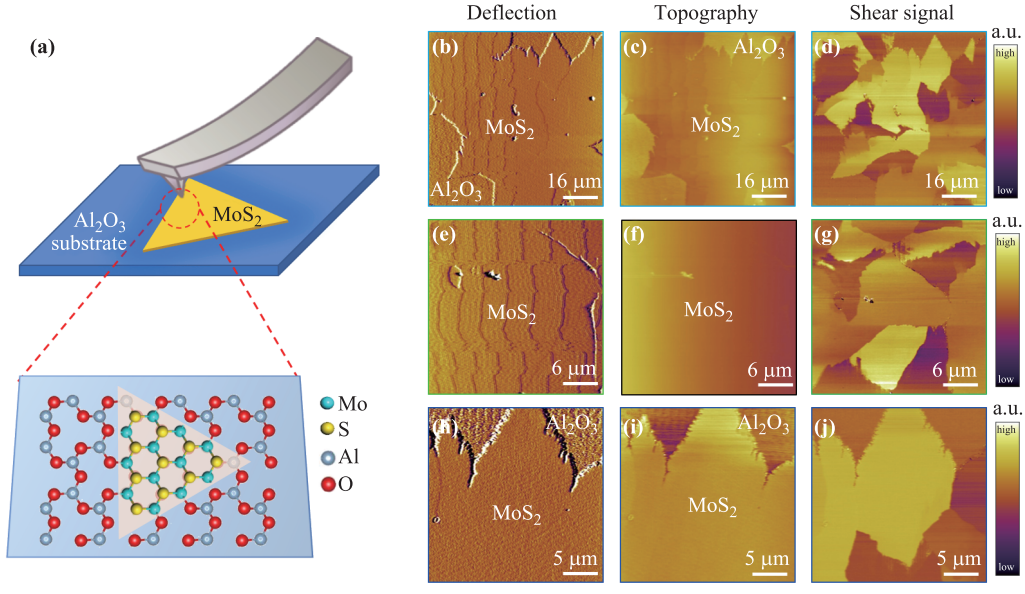


Fig. 5 AFM characterization of the CVD-grown MoS_2 monolayer on the Al_2O_3 substrate. **(a)** Schematic showing the AFM imaging of MoS_2 monolayer on the atomically flat crystalline Al_2O_3 substrate. **(b–j)** The AFM deflection (b, e, h), topography (c, f, j) and TSM shear signal (d, g, j) images of the MoS_2 monolayer on the Al_2O_3 substrate. Many terraces with step edges of the crystalline substrate were clearly observed in the deflection images. The MoS_2 grains clearly visualized in the TSM images.

films, as shown in Figs. 4(e) and (h). The crystalline domains of the top layer graphene were clearly observed, while no bilayer regions marked by the white dashed lines were resolved. We can directly conclude that the second graphene layer is underlying the first layer, confirm the underlying growth model of bilayer graphene [36].

The previous TSM measurements of 2D materials were performed on the amorphous SiO_2/Si substrate. We found that amorphous substrate does not contribute any shear signals during the TSM imaging. While for the 2D materials on the crystalline substrates, whether the TSM method is still applicable or not, should be further investigated. The MoS_2 monolayer films directly grown on the crystalline Al_2O_3 substrate were further characterized by the TSM measurements, as shown in Fig. 5. The substrate terraces with straight edges were resolved in the AFM deflection images, indicating the crystalline nature of the Al_2O_3 substrate. No crystalline MoS_2 domains were resolved in the AFM topography and deflection images, but in the TSM images. Then we can conclude that the underlying crystalline substrate does not apparently contribute to the TSM shear signal comparing to the 2D layers with the puckering effect, and the TSM characterization can be generalized to 2D materials on the crystalline substrates.

In summary, we have identified the toplayer-dependent crystallographic orientation imaging of 2D materials, which enable the crystallographic orientation imaging of bilayer films with transverse shear microscopy. We experimentally demonstrate that only the top layer MoS_2 was crystallographic orientation imaged with TSM, which will be useful in the twist bilayer systems. The unique intercalation growth mode of the second layer graphene during the CVD growth process was confirmed with the toplayer-dependent TSM characterization and SKPM measurements. The crystallographic orientation imaging of MoS_2 monolayer on the crystalline Al_2O_3 substrate was further realized and demonstrated the general applications of the TSM method. Our research will be beneficial in understanding the nanomechanical behaviors of 2D systems and provides a convenient and powerful approach to facilitate the nondestructive crystallographic orientation characterization of various 2D atomic crystal systems.

Electronic supplementary material The data that support the findings of this study are available within the article and its supplementary materials, which are available in the online version of this article at https://doi.org/10.1007/s11467-021-1072-y and https://journal.hep.com.cn/fop/EN/10.1007/s11467-021-1072-y and are accessible for authorized users.

Acknowledgements This work was supported by the National Natural Science Foundation of China (NSFC, Grant Nos. 21622304, 61674045, and 11604063), Ministry of Science and Technology (MOST) of China (Grant No. 2016YFA0200700), Strategic Priority Research Program, Key Research Program of Frontier Sciences and Instrument Developing Project of Chinese Academy of Sciences (CAS; Grant Nos. XDB30000000, QYZDB-SSW-SYS031, and YZ201418), Grant-in-Aid for Scientific Research from Japan Society for the Promotion of Science (JSPS) from the Ministry of Education, Culture, Sports, Science, and Technology of Japan (Grant Nos. JP16H06327, JP16H06504, JP17H01061, and JP17H010610), and Osaka University's International Joint Research Promotion Program (Grant Nos. J171013014, J171013007, J181013006, and Ja19990011). Z. H. Cheng was supported by Distinguished Technical Talents Project and Youth Innovation Promotion Association CAS, the Fundamental Research Funds for the Central Universities, and the Research Funds of Renmin University of China (Grant No. 18XNLG01). S. Chen appreciate the support from Beijing Natural Science Foundation (Grant No. 2192024).

References

1. K. S. Novoselov, A. K. Geim, S. V. Morozov, D. Jiang, Y. Zhang, S. V. Dubonos, I. V. Grigorieva, and A. A. Firsov, Electric field effect in atomically thin carbon films, *Science* 306(5696), 666 (2004)
2. C. Dang, M. Guan, S. Hussain, W. Wen, Y. Zhu, L. Jiao, S. Meng, and L. Xie, Phase transition photodetection in charge density wave tantalum disulfide, *Nano Lett.* 20(9), 6725 (2020)
3. A. Gupta, T. Sakthivel, and S. Seal, Recent development in 2D materials beyond graphene, *Prog. Mater. Sci.* 73, 44 (2015)
4. S. Zhang, T. Ma, A. Erdemir, and Q. Li, Tribology of two-dimensional materials: From mechanisms to modulating strategies, *Mater. Today* 26, 67 (2019)
5. S. Li, Q. Li, R. W. Carpick, P. Gumbsch, X. Z. Liu, X. Ding, J. Sun, and J. Li, The evolving quality of frictional contact with graphene, *Nature* 539(7630), (2016)
6. R. Wang, X. G. Ren, Z. Yan, L. J. Jiang, W. E. I. Sha, and G. C. Shan, Graphene based functional devices: A short review, *Front. Phys.* 14(1), 13603 (2019)
7. J. Mao, Y. Wang, Z. Zheng, and D. Deng, The rise of two-dimensional MoS_2 for catalysis, *Front. Phys.* 13(4), 138118 (2018)
8. S. Hussain, R. Xu, K. Xu, L. Lei, L. Meng, Z. Zheng, S. Xing, J. Guo, H. Dong, A. Liaqat, M. A. Iqbal, Y. J. Li, Y. Sugawara, F. Pang, W. Ji, L. Xie, and Z. Cheng, Strain-induced hierarchical ripples in MoS_2 layers investigated by atomic force microscopy, *Appl. Phys. Lett.* 117(15), 153102 (2020)
9. R. Xu, F. Pang, Y. Pan, Y. Lun, L. Meng, Z. Zheng, K. Xu, L. Lei, S. Hussain, Y. J. Li, Y. Sugawara, J. Hong, W. Ji, and Z. Cheng, Atomically asymmetric inversion scales up to mesoscopic single-crystal monolayer flakes, *ACS Nano* 14(10), 13834 (2020)
10. J. H. Kim, J. H. Jeong, N. Kim, R. Joshi, and G. H. Lee, Mechanical properties of two-dimensional materials and their applications, *J. Phys. D Appl. Phys.* 52(8), 083001 (2019)

11. S. Ye, K. Xu, L. Lei, S. Hussain, F. Pang, X. Liu, Z. Zheng, W. Ji, X. Shi, R. Xu, L. Xie, and Z. Cheng, Nanoscratch on single-layer MoS_2 crystal by atomic force microscopy: semi-circular to periodical zigzag cracks, *Mater. Res. Express* 6(2), 025048 (2018)
12. H. Li, X. Duan, X. Wu, X. Zhuang, H. Zhou, Q. Zhang, X. Zhu, W. Hu, P. Ren, P. Guo, L. Ma, X. Fan, X. Wang, J. Xu, A. Pan, and X. Duan, Growth of alloy $MoS_{2x}Se_{2(1-x)}$ nanosheets with fully tunable chemical compositions and optical properties, *J. Am. Chem. Soc.* 136(10), 3756 (2014)
13. W. Chen, E. J. Santos, W. Zhu, E. Kaxiras, and Z. Zhang, Tuning the electronic and chemical properties of monolayer MoS_2 adsorbed on transition metal substrates, *Nano Lett.* 13(2), 509 (2013)
14. Q. H. Wang, K. Kalantar-Zadeh, A. Kis, J. N. Coleman, and M. S. Strano, Electronics and optoelectronics of two-dimensional transition metal dichalcogenides, *Nat. Nanotechnol.* 7(11), 699 (2012)
15. M. A. Iqbal, A. Liaqat, S. Hussain, X. Wang, M. Tahir, Z. Urooj, and L. Xie, Ultralow-transition-energy organic complex on graphene for high-performance shortwave infrared photodetection, *Adv. Mater.* 32(37), 2002628 (2020)
16. B. Tang, S. Hussain, R. Xu, Z. Cheng, J. Liao, and Q. Chen, Novel type of synaptic transistors based on a ferroelectric semiconductor channel, *ACS Appl. Mater. Interfaces* 12(22), 24920 (2020)
17. M. A. Iqbal, M. Cui, A. Liaqat, R. Faiz, M. Hossain, X. Wang, S. Hussain, C. Dang, H. Liu, W. Wen, J. Wu, and L. Xie, Organic charge transfer complexes on graphene with ultrahigh near infrared photogain, *Nanotechnology* 30(25), 254003 (2019)
18. Y. Sun, J. Pan, Z. Zhang, K. Zhang, J. Liang, W. Wang, Z. Yuan, Y. Hao, B. Wang, J. Wang, Y. Wu, J. Zheng, L. Jiao, S. Zhou, K. Liu, C. Cheng, W. Duan, Y. Xu, Q. Yan, and K. Liu, Elastic properties and fracture behaviors of biaxially deformed, polymorphic $MoTe_2$, *Nano Lett.* 19(2), 761 (2019)
19. V. Kalihari, G. Haugstad, and C. D. Frisbie, Distinguishing elastic shear deformation from friction on the surfaces of molecular crystals, *Phys. Rev. Lett.* 104(8), 086102 (2010)
20. A. W. Tsen, L. Brown, M. P. Levendorf, F. Ghahari, P. Y. Huang, R. W. Havener, C. S. Ruiz-Vargas, D. A. Muller, P. Kim, and J. Park, Tailoring electrical transport across grain boundaries in polycrystalline graphene, *Science* 336(6085), 1143 (2012)
21. C. Lee, X. Wei, J. W. Kysar, and J. Hone, Measurement of the elastic properties and intrinsic strength of monolayer graphene, *Science* 321(5887), 385 (2008)
22. H. Wang, E. J. Sandoz-Rosado, S. H. Tsang, J. Lin, M. Zhu, G. Mallick, Z. Liu, and E. H. T. Teo, Elastic properties of 2D ultrathin tungsten nitride crystals grown by chemical vapor deposition, *Adv. Funct. Mater.* 29(31), 1902663 (2019)
23. S. Zhang, Y. Hou, S. Li, L. Liu, Z. Zhang, X. Q. Feng, and Q. Li, Tuning friction to a superlubric state via in-plane straining, *Proc. Natl. Acad. Sci. USA* 116(49), 24452 (2019)
24. L. Lei, R. Xu, S. Ye, X. Wang, K. Xu, S. Hussain, Y. J. Li, Y. Sugawara, L. Xie, W. Ji, and Z. Cheng, Local characterization of mobile charge carriers by two electrical AFM modes: Multi-harmonic EFM versus sMIM, *J. Chem. Phys.* 2, 025013 (2018)
25. K. Xu, S. Ye, L. Lei, L. Meng, S. Hussain, Z. Zheng, H. Zeng, W. Ji, R. Xu, and Z. Cheng, Dynamic interfacial mechanical-thermal characteristics of atomically thin two-dimensional crystals, *Nanoscale* 10(28), 13548 (2018)
26. Z. Zheng, R. Xu, S. Ye, S. Hussain, W. Ji, P. Cheng, Y. Li, Y. Sugawara, and Z. Cheng, High harmonic exploring on different materials in dynamic atomic force microscopy, *Sci. China Technol. Sci.* 61(3), 446 (2018)
27. Z. Y. Zheng, R. Xu, K. Q. Xu, S. L. Ye, F. Pang, L. Lei, S. Hussain, X. M. Liu, W. Ji, and Z. Cheng, Real-space visualization of intercalated water phases at the hydrophobic graphene interface with atomic force microscopy, *Front. Phys.* 15(2), 23601 (2020)
28. M. Campione and E. Fumagalli, Friction anisotropy of the surface of organic crystals and its impact on scanning force microscopy, *Phys. Rev. Lett.* 105(16), 166103 (2010)
29. J. S. Choi, J. S. Kim, I. S. Byun, D. H. Lee, M. J. Lee, B. H. Park, C. Lee, D. Yoon, H. Cheong, K. H. Lee, Y. W. Son, J. Y. Park, and M. Salmeron, Friction anisotropy-driven domain imaging on exfoliated monolayer graphene, *Science* 333(6042), 607 (2011)
30. Q. Li, C. Lee, R. W. Carpick, and J. Hone, Substrate effect on thickness-dependent friction on graphene, *Phys. Status Solidi. B* 247(5), 2909–2914 (2010)
31. K. Xu, Y. Pan, S. Ye, L. Lei, S. Hussain, Q. Wang, Z. Yang, X. Liu, W. Ji, R. Xu, and Z. Cheng, Shear anisotropy-driven crystallographic orientation imaging in flexible hexagonal two-dimensional atomic crystals, *Appl. Phys. Lett.* 115(6), 063101 (2019)
32. X. Xu, T. Schultz, Z. Qin, N. Severin, B. Haas, S. Shen, J. N. Kirchhof, A. Opitz, C. T. Koch, K. Bolotin, J. P. Rabe, G. Eda, and N. Koch, Microstructure and elastic constants of transition metal dichalcogenide monolayers from friction and shear force microscopy, *Adv. Mater.* 30(39), 1803748 (2018)
33. S. Hussain, K. Xu, S. Ye, L. Lei, X. Liu, R. Xu, L. Xie, and Z. Cheng, Local electrical characterization of two-dimensional materials with functional atomic force microscopy, *Front. Phys.* 14(3), 33401 (2019)
34. J. S. Choi, Y. J. Chang, S. Woo, Y. W. Son, Y. Park, M. J. Lee, I. S. Byun, J. S. Kim, C. G. Choi, A. Bostwick, E. Rotenberg, and B. H. Park, Correlation between micrometer-scale ripple alignment and atomic-scale crystallographic orientation of monolayer graphene, *Sci. Rep.* 4(1), 7263 (2015)
35. J. S. Choi, J. S. Kim, I. Byun, D. H. Lee, I. R. Hwang, B. H. Park, T. Choi, J. Y. Park, and M. Salmeron, Facile characterization of ripple domains on exfoliated graphene, *Rev. Sci. Instrum.* 83(7), 073905 (2012)
36. H. Ying, W. Wang, W. Liu, L. Wang, and S. Chen, Layer-by-layer synthesis of bilayer and multilayer graphene on Cu foil utilizing the catalytic activity of cobalt nano-powders, *Carbon* 146, 549 (2019)

37. C. Lee, Q. Li, W. Kalb, X. Z. Liu, H. Berger, R. W. Carpick, and J. Hone, Frictional characteristics of atomically thin sheets, *Science* 328(5974), 76 (2010)

38. H. Q. Zhao, X. Mao, D. Zhou, S. Feng, X. Shi, Y. Ma, X. Wei, and Y. Mao, Bandgap modulation of MoS_2 monolayer by thermal annealing and quick cooling, *Nanoscale* 8(45), 18995 (2016)

39. M. R. Vazirisereshk, K. Hasz, M. Q. Zhao, A. T. C. Johnson, R. W. Carpick, and A. Martini, Nanoscale friction behavior of transition-metal dichalcogenides: Role of the chalcogenide, *ACS Nano* 14(11), 16013 (2020)

40. Y. Zheng, J. Chen, M. F. Ng, H. Xu, Y. P. Liu, A. Li, S. J. O'Shea, T. Dumitrica, and K. P. Loh, Quantum mechanical rippling of a MoS_2 monolayer controlled by interlayer bilayer coupling, *Phys. Rev. Lett.* 114(6), 065501 (2015)

41. H. Li, J. Tao, Y. Luo, L. Deng, and Z. Den, Exploring the evolution of passenger flow and travel time reliability with the expanding process of metro system using smartcard data, *J. Harbin Inst. Technol.* 26(1), 5 (2019)